A robust statistical framework to detect multiple sources of hidden variation in single-cell transcriptomes

Donghyung Lee[1,*], Anthony Cheng[1,2], and Duygu Ucar[1,*]

[1]The Jackson Laboratory for Genomic Medicine, Farmington, Connecticut, Unites States of America, [2]University of Connecticut Health Center, Farmington, Connecticut, Unites States of America

*Correspondence: *donghyung.lee@jax.org* and *duygu.ucar@jax.org*

Abstract

Single-cell RNA-Sequencing data often harbor variation from multiple correlated sources, which cannot be accurately detected by existing methods. Here we present a novel and robust statistical framework that can capture correlated sources of variation in an iterative fashion: iteratively adjusted surrogate variable analysis (IA-SVA). We demonstrate that IA-SVA accurately captures hidden variation in single cell RNA-Sequencing data arising from cell contamination, cell-cycle stage, and differences in cell types along with the marker genes associated with the source.

Single-cell RNA-Sequencing (scRNA-Seq) data often harbor variation from diverse sources including technical (e.g., biases in capturing transcripts from single cells, PCR amplifications) and biological factors (e.g., differences in cell cycle stage or cell types) that might confound biological conclusions [1-3]. Detecting and adjusting for hidden heterogeneity in scRNA-Seq data is essential to accurately characterize gene expression changes stemming from a biological variable of interest (e.g., disease vs. normal). A number of statistical methods have

24 been proposed to detect hidden sources of variation in microarray, bulk, and single-cell RNA-
25 Seq data: SSVA[4] (supervised surrogate variable analysis), USVA[5] (unsupervised SVA), ISVA[6]
26 (Independent SVA), RUVcp[7, 8] (removing unwanted variation using control probes), RUVres
27 (RUV using residuals), RUVemp (RUV using empirical negative controls) and scLVM[9] (single-
28 cell latent variable model). One caveat of these methods is their assumption that the multiple
29 sources of variation are uncorrelated (i.e., orthogonal) with each other and with known
30 variables[6]. However, in reality transcriptomic data especially single cell measurements typically
31 contain variation stemming from multiple yet correlated hidden factors due to poor experimental
32 design, technical limitations, or biological factors. For example, the number of expressed genes
33 in a cell (a major source of variation), experimental batch effects, cell cycle stage, cell size, and
34 cell type can be highly correlated with each other and may confound the downstream biological
35 conclusions [9, 10 11, 12]. To properly detect and account for these sources of variation, we
36 developed a robust and iterative statistical framework, IA-SVA (iteratively adjusted surrogate
37 variable analysis) (**Fig. 1a**). IA-SVA is designed to identify multiple and potentially correlated
38 hidden sources of variation from scRNA-Seq data with high statistical power and low error rate
39 (see Online Methods, **Supplementary Fig. 1**, and https://github.com/UcarLab/IA-SVA/).
40 The major advantages of IA-SVA over existing methods are three-fold: First, it
41 accurately captures multiple hidden sources of variation even if the sources are correlated.
42 Second, it enables assessing the significance of each detected factor for explaining the
43 unmodeled variation in the data. Third, it delivers marker genes that are significantly associated
44 with the detected hidden factors. Factors or marker genes inferred by IA-SVA can be
45 instrumental in data interpretation and in improving the performance of downstream analyses,

46 such as clustering/visualization of single-cell data using t-distributed stochastic neighbor
47 embedding (t-SNE) [13].

48 Using simulated scRNA-Seq data, we studied and compared the empirical Type I error
49 rate, the power of detection, and the accuracy of estimation for IA-SVA and existing state-of-the-
50 art methods, which can also infer the number of significant hidden factors (i.e., USVA and
51 SSVA) (See Online Methods). Under different simulation scenarios, we found that IA-SVA
52 consistently outperformed USVA and SSVA in terms of detection power and accuracy of the
53 estimate while controlling the Type I error rate under the nominal level (0.05) (**Fig. 1b**). In
54 particular, IA-SVA significantly outperformed alternatives when hidden factors affect a small
55 percentage of genes (10-20%) and when these factors are moderately correlated with a known
56 factor (i.e., group variable) (the first three columns of **Fig. 1b**). We compared the efficacy of IA-
57 SVA against a broader number of supervised (SSVA and RUVcp) and unsupervised (USVA,
58 PCA, RUVemp and RUVres) methods (**Supplementary Note 1)**. Similarly, IA-SVA was
59 particularly effective in estimating hidden factors that affect a subset of genes (10-20%) (Factor
60 3 in **Supplementary Fig. 2)** and in inferring correlations among factors (**Supplementary Fig.
61 3**). We also compared the performance of IA-SVA against unsupervised methods (USVA, PCA,
62 RUVemp, RUVres) to estimate the heterogeneity arising from differences in brain cell types
63 (neurons vs. oligodendrocytes) [14] (See Online Methods). IA-SVA significantly outperformed
64 other methods and accurately inferred the factor that corresponds to cell type assignments ($|r|$ =
65 0.95 vs. 0.83 for the second best performance by RUVres) (**Supplementary Fig. 4**).

66 To test the efficacy of IA-SVA in capturing variation within a relatively homogenous cell
67 population, we studied alpha cells (n=101) from three diabetic patients [15] (see Online Methods).
68 We found that Surrogate Variable 2 (SV2) inferred by IA-SVA clearly separated alpha cells into

69 two groups (six outlier cells marked in red vs. the rest at SV2 < -0.2) (**Fig. 2a**). Top 30 genes
70 (e.g., *CD9*, *SPARC, COL4A1, PMEPA1, ENG*) correlated with SV2 clearly separated alpha cells
71 into two clusters, where six outlier cells exclusively expressed these genes (**Fig. 2b**). Alternative
72 methods (PCA, USVA, tSNE) didn't clearly separate these outlier cells, especially in the case of
73 tSNE analyses (**Fig. 2a**). This heterogeneity detected in alpha cells was reproducible in a bigger
74 and independently generated islet scRNA-Seq data using the same platform [16] (**Supplementary**
75 **Fig. 5**). In both datasets this heterogeneity was associated with fibrotic response genes (e.g.,
76 *SPARC, COL4A1, COL4A2)* suggesting that these outlier cells might originate from cell
77 contamination (e.g., fibroblasts contaminating islet cells) or from cell doublets captured
78 together—a known problem in early Fluidigm C1 experiments [17, 18].

79 Another established source of heterogeneity in scRNA-Seq data is the differences in cell-
80 cycle stages [3]. To test whether IA-SVA can capture this, we analyzed scRNA-seq data obtained
81 from human glioblastomas with an established cell-cycle signature [19]. Using IA-SVA, we
82 detected a source of hidden heterogeneity (SV2) that clearly separated 12 cells from the rest (**Fig.**
83 **2c**) and identified 87 marker genes associated with this source (**Fig. 2d**). Pathway and GO
84 enrichment analyses of these marker genes [20, 21] revealed significant enrichment for cell-cycle
85 stage related GO terms and KEGG pathways (**Supplementary Fig. 6 and Supplementary**
86 **Table 1**). PCA, USVA and tSNE failed to separate these cells (**Fig. 2c**).

87 In scRNA-Seq data, technical or biological factors are often correlated and can
88 deteriorate the single cell clustering results (e.g., clustering with respect to cell types) by
89 masking the real signal or generating spurious clusters. IA-SVA can be particularly effective in
90 handling this problem by uncovering hidden factors while adjusting for all potential confounders.
91 Moreover, IA-SVA delivers marker genes associated with the hidden factor, which can be

92 further tested and evaluated for their biological relevance (e.g., novel markers for different cell
93 types) and can be utilized in clustering analyses for increased performance. To test this, we first
94 studied scRNA-Seq data from alpha (n=101), beta (n=96), and ductal (n=16) cells obtained from
95 three diabetic patients [15] (Online Methods) and used tSNE on all expressed genes to cluster these
96 cells. Color-coding based on the reported cell type assignments [15] showed that, tSNE cannot
97 effectively separate these cells into their respective categories (**Fig. 3a**). Next, we applied IA-
98 SVA on this data and focused on top two significant SVs (SV1 and SV2) since they separated
99 cells into distinct clusters (**Supplementary Fig. 7**). 86 genes were associated with these two SV2
100 that notably included previously known markers used in the original study (*INS*, *GCG*, *KRT19*)
101 and uncovered potential novel markers of islet cells (Fig. 3c). As expected, tSNE analyses on
102 these 86 genes improved the clustering results significantly and clearly separated different cell
103 types (**Fig. 3b**). Such improved clustering analyses can also help reveal cells that might be
104 incorrectly labeled based on a single gene marker. We tested whether this pattern can be
105 recapitulated in a bigger data with confounding variables[16] by analyzing transcriptomes of 1600
106 islet cells including alpha (n=946), beta (n=503), delta (n=58), and PP (n=93) cells (Online
107 Methods). In this case, designated cell type assignments correlated with known factors especially
108 with the patient identifications (C=0.48 for patient id, C=0.1 for sex, C=0.03 for phenotype and
109 C=0.25 for ethnicity, C=Pearson's contingency coefficient). If not properly adjusted for, these
110 correlations would lead to spurious clustering of cells. For example, when tSNE is performed on
111 these islet cells and cells are color-coded with respect to the original cell-type assignments [16],
112 cell types did not separate from each other and spurious clusters were observed within each cell
113 type (**Fig. 3d**). As suspected, potential confounding factors, particularly patient id and ethnicity,
114 explained the spurious clustering of cells (**Supplementary Fig. 8**). Existing methods to improve

115 scRNA-Seq clustering results (e.g., 'Spectral tSNE' [22]) regress out (remove) variation associated
116 with known variables before estimating hidden factors. However, when biological variables of
117 interest (e.g., cell type assignments) are highly correlated with known factors as in this case,
118 removing the known effects will also impact the signal of interest. To handle this, we conducted
119 IA-SVA analyses while accounting for known factors and extracted four significant SVs. Among
120 these, SV1 and SV4 grouped cells into disjoint clusters (**Supplementary Fig. 9a and b**);
121 therefore we focused on these as putative SVs associated with differences in cell types (SV3 is
122 not considered since it captures cell contamination). 57 genes associated with these two SVs
123 included once again known marker genes for islet cells (i.e., *INS* and *GCG*) (**Supplementary**
124 **Fig. 10**). tSNE analyses using these genes clearly separated different cell types into discrete
125 clusters and reinforced the importance of properly adjusting for known factors prior to clustering
126 or marker gene detection (**Figure 3e**). Top surrogate factors obtained via PCA and USVA failed
127 to detect the heterogeneity associated with cell types (**Supplementary Fig. 9c and d**).
128 In summary, IA-SVA can accurately and robustly estimate hidden sources of variation in
129 gene expression data while adjusting for known factors introducing unwanted variation. The
130 iterative framework to detect multiple and potentially correlated factors along with their
131 significance is the main advantage of IA-SVA over existing methods. This flexibility is more
132 realistic given the confounded nature of known and unknown factors introducing heterogeneity
133 in gene expression levels particularly in scRNA-Seq data. Furthermore, IA-SVA infers marker
134 genes associated with the source of variation that can be used for various purposes including
135 novel marker gene detection for different cell types.
136

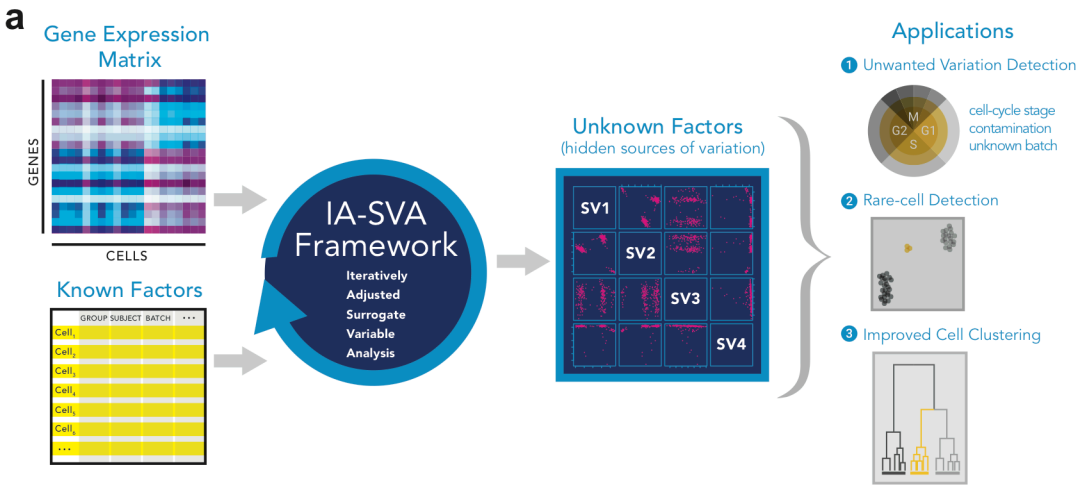

b

	USVA	SSVA	IA-SVA	USVA	SSVA	IA-SVA
	|r| = 0.3 ~ 0.6			|r|<0.3		
Power*(F1**)	1	1	1	1	1	1
Power (F2)	1	1	1	1	1	1
Power (F3)	0.78	0.78	0.87	1	1	1
Cor***(F1)	0.93	0.95	0.95	0.98	0.98	1
Cor (F2)	0.72	0.75	0.94	0.94	0.94	0.99
Cor (F3)	0.75	0.78	0.95	0.93	0.93	0.98

	USVA	SSVA	IA-SVA
Type I error*	0.09	0.09	0.04

* Nominal Type I error rate: 0.05
** F1, F2, F3 refers to Factor1, Factor2, and Factor 3
*** Average of the absolute Pearson correlation coefficient between the true factor and the estimated factor is used as the accuracy measure.

Figure 1. IA-SVA is a robust statistical framework to detect sources of hidden heterogeneity. (a) IA-SVA uses single-cell gene expression data matrix and known factors to detect hidden sources of variation (e.g., cell contamination, cell-cycle status, and cell type). These hidden factors can be used as additional covariates in differential analysis to increase statistical power. If these factors match to a biological variable of interest (e.g., cell type assignment), genes highly correlated with the factor can be detected and used in downstream analyses (e.g., clustering). **(b)** Empirical Type I error rate, detection power and the accuracy of estimates for IA-SVA, SSVA, and USVA using simulated single-cell gene expression data. Alternative scenarios are simulated in which hidden factors are moderately ($|r|$=~0.3-0.6, first three columns) or weakly ($|r|$<0.3, last three columns) correlated with the group variable.

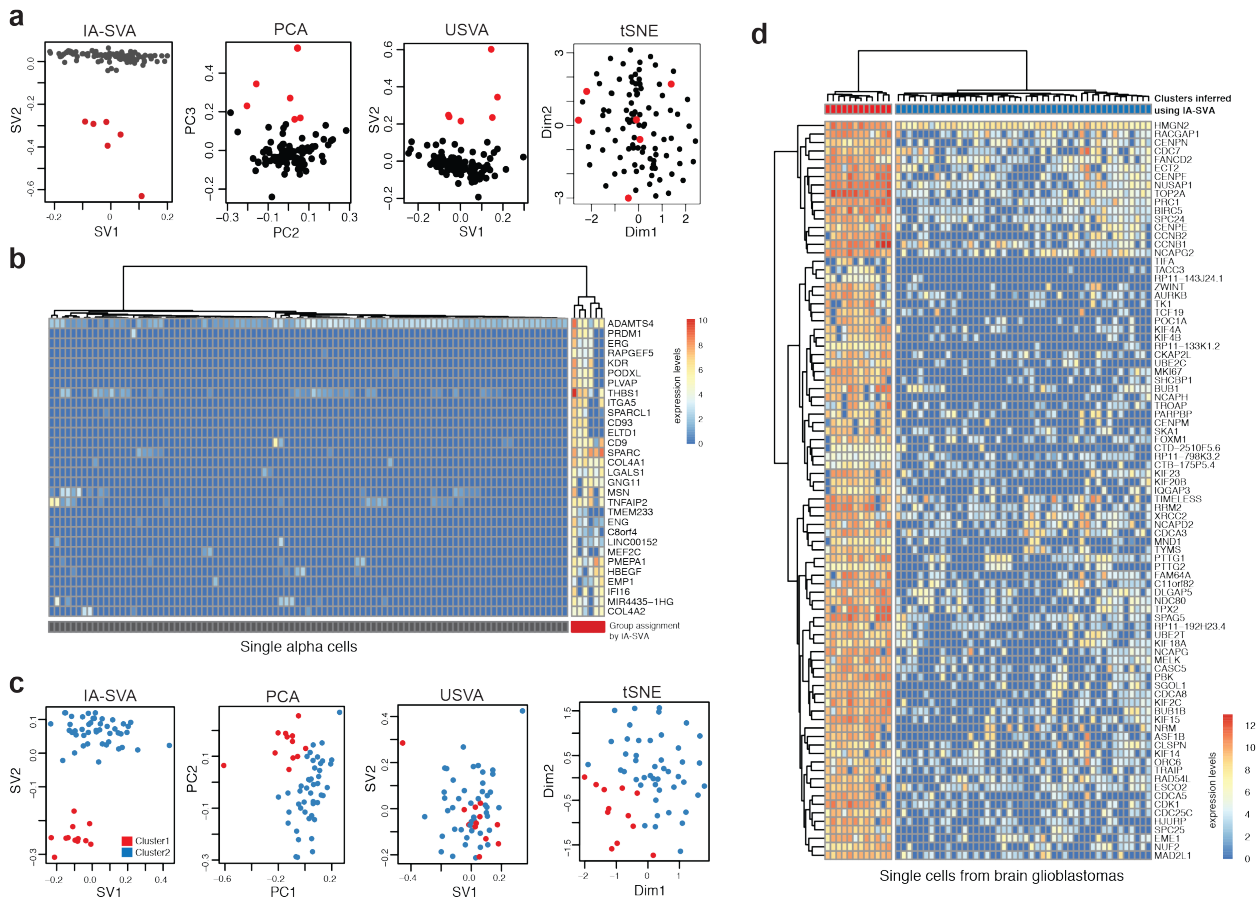

Figure 2. IA-SVA can detect heterogeneity originated from a few cells. (a) Heterogeneity within alpha cells captured using IA-SVA, PCA, USVA, and tSNE. Cells are clustered into two groups (black vs. red dots) based on IA-SVA's surrogate variable 2 (SV2 < -0.2). In PCA, PC1 was discarded since it explains the number of expressed genes. (**b**) Hierarchical clustering of alpha cells using the top 30 marker genes (ward.D2 and cutree_cols =2). 6 cells clearly separated from the rest of the cells in terms of the expression of these 30 genes. (**c**) Heterogeneity detected within glioblastomas using IA-SVA, PCA, USVA, and tSNE. IA-SVA's SV2 clearly separates cells into two groups (blue vs. red dots, SV2 < -0.1) with respect to their cell cycle stages. Other methods failed to detect this cell-cycle related heterogeneity. **(d)** Hierarchical clustering on 87 marker genes confirms the separation of cells based on these markers (ward.D2 and cutree_cols = 2).

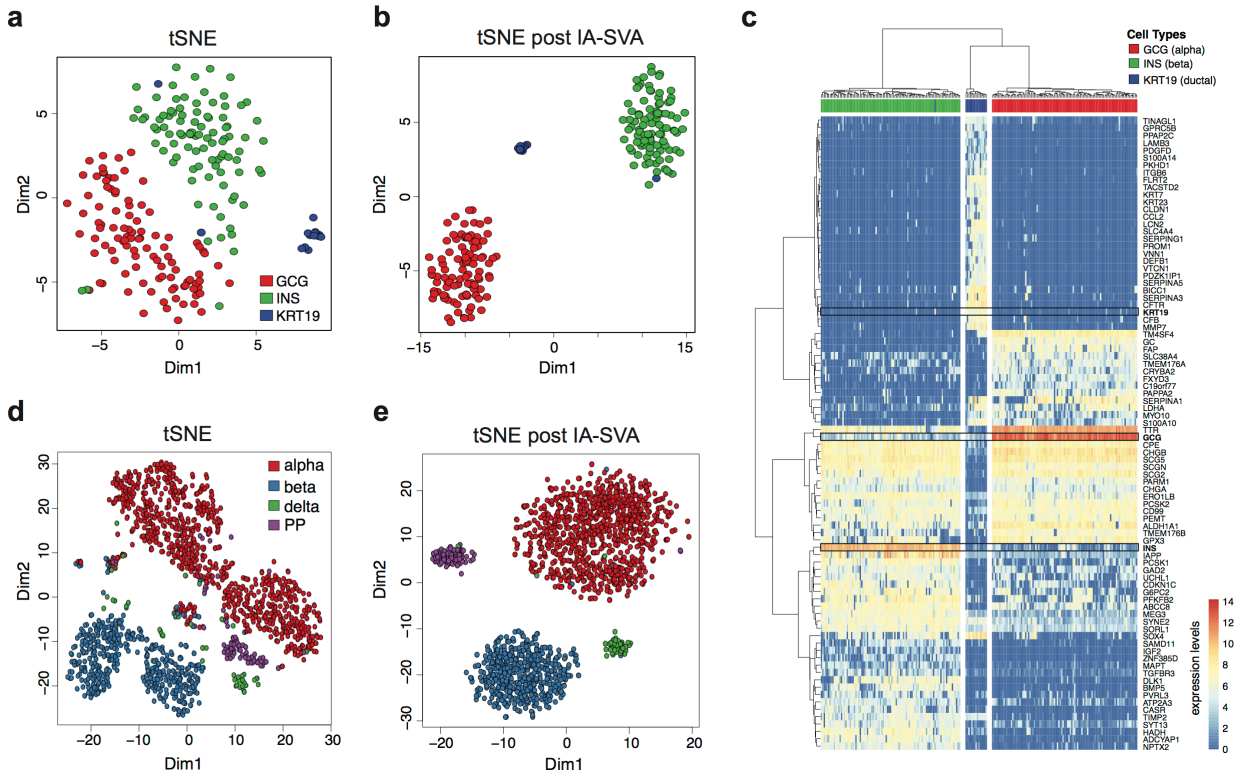

Fig. 3. IA-SVA based marker gene selection enhances the performance of clustering algorithms. (a) tSNE analyses using all expressed genes in human islet data. Cells are color-coded based on original cell-type assignments. (**b**) tSNE analyses using IA-SVA marker genes (n=86). Note the improved clustering of cell types into discrete clusters. (**c**) Hierarchical clustering using 86 marker genes clearly separate cell types (ward.D2 and cutree_cols=3). Rows marked with boxes refer to marker genes used in the original study. (**d**) tSNE analyses using all expressed genes in a bigger islet data. Note that cells are not effectively clustered with respect to their assigned cell types. (**e**) tSNE analyses using marker genes obtained via IA-SVA (n=57). Note the improved clustering of cells into discrete clusters.

ACCESSION CODES

The single-cell RNA sequencing read counts and annotations describing samples and experiment settings are included in an R data package ("iasvaExamples") containing data examples for IA-SVA (https://github.com/dleelab/iasvaExamples).

ACKNOWLEDGMENTS

This work has been supported by the Jackson Laboratory (JAX) for Genomic Medicine start-up funds (to D.U.) and the Jackson Laboratory Scientific Services Innovation Fund (to D.L. and D.U.). We thank JAX Computational Science group, Ucar and Stitzel lab members for constructive feedback throughout this project. We thank Jane Cha, JAX scientific illustrator, for her help with the figures.

AUTHOR CONTRIBUTIONS

D.L. and D.U. designed the project, generated the figures and wrote the manuscript. D.L. developed the statistical framework and run the data analyses. A.C. contributed to the data pre-processing and the generation of the R package. All authors read and approved this manuscript.

COMPETING FINANCIAL INTERESTS

The authors declare no competing financial interests.

201 **ONLINE METHODS**

202 **IA-SVA framework.** Formally, we model the log-transformed sequencing read counts for *m*
203 genes and *n* samples (*i.e.,* $m \times n = Y$) as a combination of primary variable of interest, known
204 and unknown sources of variation as follows:

205 $$Y_{m\times n} = X_{m\times p}\beta_{p\times n} + Z_{m\times q}\gamma_{q\times n} + W_{m\times k}\delta_{k\times n} + \varepsilon_{m\times n},$$

206 where *X* is a matrix for *p* primary variable(s) of interest (e.g., group assignment for cases and
207 controls), *Z* is a matrix for *q* known factors (e.g., sex or ethnicity), *W* is a matrix for *k* unknown
208 factors and ε is the error term. With this model, we can account for any clinical/experimental
209 information about samples (e.g., sex, ethnicity, age, BMI, experimental batch) as known factors
210 (*Z*) and dissect the variation in the read count data that is attributable to hidden factors (*W*).

211 Existing unsupervised methods (e.g., USVA, RUVres, ISVA) obtain the residual matrix
212 by regressing read counts (*Y*) on all known factors (*X* and *Z*). Then, they infer the number of
213 hidden factors and directly estimate hidden factors from the residual matrix using dimensionality
214 reduction algorithms (e.g., principal component analysis (PCA), singular value decomposition
215 (SVD) or independent component analysis (ICA)) under the assumption that hidden factors are
216 uncorrelated with each other and also with the known factors. Consequently, when this
217 assumption is not met, the direct inference from the residual matrix can lead to biased estimates
218 of hidden factors and distort estimates.

219 In contrast, IA-SVA does not impose the assumption of uncorrelated factors. Instead, it
220 allows correlations between factors to accurately estimate hidden factors via a novel iterative
221 approach. At each iteration, IA-SVA obtains residuals, i.e., read counts adjusted for all known
222 factors (*X* and *Z*) including unknown factors (surrogate variables) estimated from previous
223 iterations and extracts the principal component (PC1) from the residuals using SVD. Next it tests

224 the significance of PC1 in terms of its contribution to the unmodeled variation (i.e., the variation
225 of residuals). Using this PC1 (as in the case of previous methods) as a surrogate variable assumes
226 known factors and hidden factors are not correlated. Therefore, IA-SVA uses PC1 to infer
227 marker genes associated with the hidden factor by taking advantage of the fact that PC1 and the
228 true hidden factor are highly correlated. To detect these marker genes, IA-SVA regresses Y on
229 PC1 and calculates the coefficient of determination (R^2) for each gene. Genes with high R^2 scores
230 are considered as marker genes associated with the hidden factor. These genes are used for an
231 unbiased inference of the hidden factor. For this, IA-SVA weighs all genes with respect to their
232 R^2 scores, conducts SVD on the weighted read count matrix to obtain an unbiased PC1, and use
233 this PC1 as a surrogate variable (SV) for the hidden factor. In the next iteration, IA-SVA uses
234 this SV as an additional known factor to identify further significant hidden factors. The iterative
235 procedure of IA-SVA composed of six major steps as summarized in **Supplementary Figure 1**
236 and below:
237
238 **[Step 1]** Regress Y on all known factors (X and Z), including a surrogate variable (SV) obtained
239 from the previous iteration, to obtain residuals.
240 **[Step 2]** Conduct SVD on the obtained residuals to extract the first PC (PC1).
241 **[Step 3]** Test the significance of the contribution of PC1 to unexplained variation in the read
242 count matrix *(Y)* using a non-parametric permutation-based assessment [5, 23, 24]. For more details,
243 see next section.
244 **[Step 4]** If PC1 is significant, regress Y (in this case not using the known variables) on PC1 to
245 compute the coefficient of determination (R^2) for every gene. If PC1 is not significant, stop the
246 iteration and conduct subsequent down stream analysis using previously obtained significant

247 SVs.

248 **[Step 5]** Weigh each gene in Y with respect to its R^2 value by multiplying a gene's read counts
249 with its R^2 values. The highly weighted genes in this framework serve as the marker genes for the
250 hidden factor.

251 **[Step 6]** Conduct a second SVD on this weighted Y to obtain the first PC, which will be used as
252 the surrogate variable (SV) for the hidden factor.

253

254 At the end of this six-step procedure, if a significant SV is obtained, IA-SVA uses this SV as an
255 additional known factor in Step 1 of the next iteration. The algorithm stops, when no more
256 significant hidden factor are detected in Step 3. Significant SVs obtained via IA-SVA can be
257 used in subsequent analyses. For instance, in differential gene expression analyses SVs can be
258 added as covariates in a regression model to adjust for the unwanted variation. If SVs explain
259 biological variables of interest, e.g., cell type assignments, marker genes for SVs can be further
260 utilized (e.g., marker genes for different cell types).

261

262 **Assessing the significance of the contribution of a hidden factor in the variation of**
263 **residuals.** To assess the significance of a putative hidden factor (i.e., PC1 obtained from Step 2
264 in the previous section), we used the permutation based significance test applied in the surrogate
265 variable analysis [5, 23]. Unlike SVA, which tests all putative hidden factors at once, IA-SVA
266 assesses the significance of hidden factors one at a time during the corresponding iteration.
267 Briefly, IA-SVA i) conducts SVD on the residual matrix obtained from Step 1, ii) computes the
268 proportion of variation in this matrix explained by the first singular vector and iii) compares it

269 against the values obtained from permuted residual matrices. The detailed steps of the algorithm
270 are as follows:
271
272 **[Step 1]** Conduct SVD on the residual matrix.
273 **[Step 2]** Calculate the proportion of the variance in the residual matrix explained by the first
274 singular vector using the test statistic: $T_{obs} = \frac{\lambda_1^2}{\sum_k \lambda_k^2}$, where λ_k is the *k*-th singular value.
275 **[Step 3]** Generate a permuted residual matrix by i) permuting each row of the log-transformed
276 read count matrix *Y* and regressing *Y* on all known factors (*X* and *Z*) to obtain fitted residuals.
277 **[Step 4]** Repeat Step 3 *M* times and generate an empirical null distribution of the test statistics by
278 calculating $(T_i^0, i = 1, \ldots, M)$ for the *M* permuted residual matrices.
279 **[Step 5]** Compute the empirical p-value for the first singular vector (i.e., putative hidden factor)
280 by counting the number of times the null statistics (T_i^0) exceeds the observed one (T_{obs}) divided
281 by the number of permutations (*M*).
282
283 **Gene expression data filtering.** We filtered out low-expressed genes with read counts <= 5 in
284 less than three cells and log-transformed the retained gene expression counts for further analyses.
285
286 **Single-cell RNA-Seq data simulations**. We simulated single-cell gene expression data with
287 attributes similar to real-world scRNA-Seq data generated from human pancreatic islets [15]. We
288 first estimated zero-inflated negative binomial model parameters (i.e., p_0: probabilities that the
289 count will be zero, mu: mean of the negative binomial, size: size of the negative binomial) from
290 this data using the Polyester R package [25]. With these model parameters, we simulated
291 expression data for *m* expressed genes and *n* cells under two hypotheses: 1) the null hypothesis:

292 no hidden sources of variation, and 2) the alternative hypothesis: three hidden factors simulated
293 in the data. Under both scenarios, we simulated a primary variable of interest (i.e., case vs.
294 control) and simulated 10% of genes to be differentially expressed between the two groups.
295 Under the alternative hypothesis, we simulated three hidden factors that affect 30%, 20% and
296 10% of randomly chosen genes respectively and simulated two different scenarios where these
297 factors are moderately correlated ($|r|$=~0.3-0.6) or weakly correlated ($|r|$<0.3) with the group
298 variable.
299
300 **Detection power, Type I error rate and accuracy assessment.** To assess the detection power,
301 Type I error rate, and the accuracy of IA-SVA estimates, we simulated 1,000 times scRNA-Seq
302 data (as explained in the previous section) for 10,000 genes and 50 cells, under the null
303 hypothesis (i.e., a group (case/control) variable affecting 10% of genes and no hidden factor) and
304 under the alternative hypothesis (i.e., a group variable and three hidden factors affecting 10%,
305 30%, 20%, 10% of genes, respectively). Under the alternative hypothesis, we considered two
306 correlation scenarios where the three hidden factors are moderately ($|r|$=~0.3-0.6) or weakly
307 ($|r|$<0.3) correlated with the group variable. We used 0.05 as the nominal significance level (α).
308 Accordingly, for USVA and SSVA analyses, we set α at 0.05 by modifying the *'num.sv'*
309 function in the svaseq R package[4]. 50 permutations were used to test the significance of a
310 factor's contribution to the unexplained variation in the data. We defined the empirical Type I
311 error rate as the number of times each method detects a false positive factor under the null
312 hypothesis (i.e., a factor does not exist but is detected as significant at the nominal p-value
313 threshold of 0.05) divided by the number of simulations (i.e., 1,000). Similarly, the empirical
314 power rate for detecting a hidden factor is defined as the number of times each method detects a

315 simulated factor under the alternative hypothesis (i.e., a factor actually exists and is detected as
316 significant by the method) divided by 1,000. We assessed the accuracy of the estimates using the
317 average of the absolute correlation coefficients between the simulated and estimated hidden
318 factors.
319
320 **Inference of cell types from brain cells.** For a more realistic assessment of algorithms, we used
321 gene expression profiles of neurons (n=52) and oligodendrocytes (n=20) obtained from two
322 different brain tissues: cortex (n=65) and hippocampus (n=7) [14]. We treated the cell type
323 assignments (neuron vs. oligodendrocyte) as an unknown variable and estimated it by computing
324 the top SV (or PC in case of PCA) using IA-SVA and other unsupervised methods (i.e., USVA,
325 PCA, RUVemp and RUVres). Given that neurons and oligodendrocytes have very different
326 expression profiles, if entire genes are used for this analysis, all methods will deliver perfect
327 estimates. Thus, to enable performance comparisons, we made the problem more challenging by
328 randomly choosing 1,000 genes and considering only these genes in the analyses (same random
329 set of genes used for all methods for comparability). The number of expressed genes in each cell
330 is a major source of cell-to-cell variation in scRNA-Seq data and frequently correlates with other
331 factors [12]. Thus, 'Sample ID' and the number of expressed genes are included into IA-SVA,
332 USVA and RUVres models as known factors. We assessed the accuracy of each method in
333 inferring the true cell type by calculating the absolute Pearson correlation coefficient ($|r|$)
334 between inferred cell types and an indicator variable for the true cell type (e.g., taking one for
335 neurons and zero for oligodendrocytes).
336

337 **Detection of a subset of alpha cells that uniquely express a subset of genes.** To test whether
338 IA-SVA is effective in capturing heterogeneity within a relatively homogenous cell population,
339 we studied islet alpha cells (n=101) from three diabetic patients [15]. After filtering weakly
340 expressed genes, 14,416 genes out of 26,616 were used for further analyses. 'Patient ID' and
341 geometric library size are modeled as known factors, and top 3 significant factors contributing to
342 the unexplained variation are inferred using IA-SVA at p-value of 0.05 using 50 permutations.
343 For comparison, we applied PCA, USVA, and tSNE on this data. In the USVA analysis, we
344 similarly used 'Patient ID' and the geometric library size as known factors. In the PCA analysis,
345 PC1 is discarded since it is highly correlated with the number of expressed genes. To test
346 whether the heterogeneity detected in alpha cells is reproducible, we conducted similar analyses
347 on a bigger human islet scRNA-Seq dataset independently generated with the Fluidigm C1
348 platform [16]. We used gene expression profiles of 563 alpha cells from six diabetic patients. After
349 removing weakly expressed genes, 17,025 genes were retained. 'Patient ID' and the geometric
350 library size are modeled as known factors in our models, and top 3 significant SVs are obtained
351 using IA-SVA. For comparison, we conducted similar analyses using PCA (PC1 and PC2 are
352 discarded since PC1 matched number of expressed genes and PC2 captured the 'Patient ID',
353 which are adjusted for in IA-SVA and USVA), USVA and tSNE. For USVA, similarly, we
354 adjusted for 'Patient ID' and the geometric library size.
355
356 **Detection of heterogeneity stemming from cell-cycle stage differences**. To assess the
357 performance of IA-SVA and existing methods in detecting the effect of cell-cycle stage, we
358 analyzed scRNA-Seq data obtained from human glioblastomas, which has an established cell-
359 cycle signature [19]. We considered gene expression read counts of 25,415 genes and 58 cells

360 obtained from a tumor sample (MGH30). After filtering out lowly expressed genes, 21,151 genes
361 were retained. Using IA-SVA, we adjusted for geometric library size at the initial step and
362 iteratively extracted top 3 significant SVs at p-value of 0.05 using 50 permutations. For
363 comparison, we applied PCA, USVA and tSNE on this data. In USVA, similarly, we adjusted for
364 geometric library size.
365
366 **IA-SVA based gene selection can improve the performance of clustering algorithms.** To
367 compare the performance of tSNE combined with IA-SVA against standard tSNE analyses, we
368 studied gene expression profiles of alpha (n=101, marked with glucagon (*GCG*) expression), beta
369 (n=96, marked with insulin (*INS*) expression), and ductal (n=16, marked with *KRT19* expression)
370 cells obtained from three diabetic patients [15]. We filtered out low-expressed genes and retained
371 16,047 genes for further analyses. Then, we performed IA-SVA based marker gene selection and
372 conducted tSNE on these selected genes. For comparison we also performed tSNE on all
373 expressed genes (n=16,047). We repeated similar analyses on a bigger and more complex data
374 generated using Fluidigm C1 platform [16], which contains 1,600 cells (alpha (n=946), beta
375 (n=503), delta (n=58) and PP (n=93)) obtained from 6 diabetic and 12 non-diabetic individuals.
376 After filtering lowly expressed genes, the number of retained genes was 19,226. We first
377 clustered these 1,600 cells by performing tSNE on all expressed genes (n=19,226). Next, we
378 conducted IA-SVA analyses while accounting for the known factors (i.e., Patient ID, Phenotype
379 (diabetic vs. non-diabetic), sex and geometric library size) and performed tSNE analysis on the
380 marker genes inferred by IA-SVA.
381
382 **References**

383 1. Tung, P.-Y. et al. Batch effects and the effective design of single-cell gene expression
384 studies. *bioRxiv*, 062919 (2016).
385 2. Kowalczyk, M.S. et al. Single-cell RNA-seq reveals changes in cell cycle and
386 differentiation programs upon aging of hematopoietic stem cells. *Genome research*
387 **25**, 1860-1872 (2015).
388 3. Stegle, O., Teichmann, S.A. & Marioni, J.C. Computational and analytical challenges in
389 single-cell transcriptomics. *Nat Rev Genet* **16**, 133-145 (2015).
390 4. Leek, J.T. svaseq: removing batch effects and other unwanted noise from sequencing
391 data. *Nucleic Acids Res* **42** (2014).
392 5. Leek, J.T. & Storey, J.D. A general framework for multiple testing dependence. *Proc*
393 *Natl Acad Sci U S A* **105**, 18718-18723 (2008).
394 6. Teschendorff, A.E., Zhuang, J. & Widschwendter, M. Independent surrogate variable
395 analysis to deconvolve confounding factors in large-scale microarray profiling
396 studies. *Bioinformatics* **27**, 1496-1505 (2011).
397 7. Risso, D., Ngai, J., Speed, T.P. & Dudoit, S. Normalization of RNA-seq data using factor
398 analysis of control genes or samples. *Nat Biotechnol* **32**, 896-902 (2014).
399 8. Gagnon-Bartsch, J.A. & Speed, T.P. Using control genes to correct for unwanted
400 variation in microarray data. *Biostatistics* **13**, 539-552 (2012).
401 9. Buettner, F. et al. Computational analysis of cell-to-cell heterogeneity in single-cell
402 RNA-sequencing data reveals hidden subpopulations of cells. *Nat Biotechnol* **33**,
403 155-160 (2015).
404 10. Ilicic, T. et al. Classification of low quality cells from single-cell RNA-seq data.
405 *Genome Biol* **17**, 29 (2016).
406 11. McDavid, A., Finak, G. & Gottardo, R. The contribution of cell cycle to heterogeneity
407 in single-cell RNA-seq data. *Nat Biotechnol* **34**, 591-593 (2016).
408 12. Hicks, S.C., Teng, M. & Irizarry, R.A. On the widespread and critical impact of
409 systematic bias and batch effects in single-cell RNA-Seq data. *bioRxiv* (2015).
410 13. Maaten, L.V.D. Accelerating t-SNE using tree-based algorithms. *J. Mach. Learn. Res.*
411 **15**, 3221-3245 (2014).
412 14. Darmanis, S. et al. A survey of human brain transcriptome diversity at the single cell
413 level. *Proc Natl Acad Sci U S A* **112**, 7285-7290 (2015).
414 15. Lawlor, N. et al. Single cell transcriptomes identify human islet cell signatures and
415 reveal cell-type-specific expression changes in type 2 diabetes. *Genome Res* (2016).
416 16. Xin, Y. et al. RNA Sequencing of Single Human Islet Cells Reveals Type 2 Diabetes
417 Genes. *Cell Metab* **24**, 608-615 (2016).
418 17. Xin, Y. et al. Use of the Fluidigm C1 platform for RNA sequencing of single mouse
419 pancreatic islet cells. *Proc Natl Acad Sci U S A* **113**, 3293-3298 (2016).
420 18. Wang, Y.J. et al. Single-Cell Transcriptomics of the Human Endocrine Pancreas.
421 *Diabetes* **65**, 3028-3038 (2016).
422 19. Patel, A.P. et al. Single-cell RNA-seq highlights intratumoral heterogeneity in
423 primary glioblastoma. *Science* **344**, 1396-1401 (2014).
424 20. Kanehisa, M., Sato, Y., Kawashima, M., Furumichi, M. & Tanabe, M. KEGG as a
425 reference resource for gene and protein annotation. *Nucleic Acids Res* **44**, D457-462
426 (2016).
427 21. Gene Ontology, C. Gene Ontology Consortium: going forward. *Nucleic Acids Res* **43**,
428 D1049-1056 (2015).

429 22. Macosko, E.Z. et al. Highly Parallel Genome-wide Expression Profiling of Individual
430 Cells Using Nanoliter Droplets. *Cell* **161**, 1202-1214 (2015).
431 23. Buja, A. & Eyuboglu, N. Remarks on Parallel Analysis. *Multivariate Behav Res* **27**,
432 509-540 (1992).
433 24. Leek, J.T. & Storey, J.D. Capturing heterogeneity in gene expression studies by
434 surrogate variable analysis. *PLoS Genet* **3**, 1724-1735 (2007).
435 25. Frazee, A.C., Jaffe, A.E., Langmead, B. & Leek, J.T. Polyester: simulating RNA-seq
436 datasets with differential transcript expression. *Bioinformatics* **31**, 2778-2784
437 (2015).
438